

Article

# The Influence of Niobium Additions on Creep Resistance of Fe-27 at. % Al Alloys

Ferdinand Dobeš<sup>1</sup>, Petr Dymáček<sup>1,2,\*</sup> and Martin Friák<sup>1,2</sup> 

<sup>1</sup> Institute of Physics of Materials, Academy of Sciences of the Czech Republic, Žižkova 22, CZ-61662 Brno, Czech Republic

<sup>2</sup> CEITEC IPM, Institute of Physics of Materials, Academy of Sciences of the Czech Republic, Žižkova 22, CZ-61662 Brno, Czech Republic

\* Correspondence: pdymacek@ipm.cz; Tel.: +420-532-290-411

Received: 3 June 2019; Accepted: 27 June 2019; Published: 30 June 2019



**Abstract:** Results of creep tests of two Fe-27 at. % Al-based alloys with additions of 2.7 and 4.8 at. % of niobium conducted in the temperature range from 650 °C to 900 °C in the authors' laboratory are presented. The purpose of the study is to supplement previous work on Fe-Al-Nb alloys to obtain a more complete overview of creep properties from the dilute alloy with 1% of Nb up to the eutectic alloy with 10% of niobium. At higher temperatures and lower stresses, the creep resistance of the 10% niobium alloy is better than that of the lower niobium alloys. On the other hand, the eutectic alloy loses its preference at lower temperatures and higher deformation rates. This phenomenon is similar to that reported by Yildirim et al. for Fe-50 at. % Al-based alloys and is probably associated with an increased stress sensitivity of the eutectic alloy.

**Keywords:** iron aluminides; creep; stress exponent; activation energy

## 1. Introduction

High-temperature creep resistance and tensile strength of Fe-Al-based alloys can be improved by additions of niobium because it contributes to both solid solution hardening and precipitation strengthening [1–5]. The effect of niobium additions on mechanical properties was to some extent studied for both ferritic alloys with Al concentrations less than 19% (all compositions are given in at. % throughout this paper) [6–10] and alloys based on ordered compounds of Fe<sub>3</sub>Al [8,9,11–17]. Recently, the influence of niobium additions to FeAl (Fe-(50-x)% Al-x% Nb, x = 1, 3, 5, 7, 9) [18], i.e., up to the eutectic through between FeAl and C14 Laves phase on room-temperature mechanical properties were studied. It was shown that the eutectic alloy with 9% Nb exhibited the lowest compressive strength among the heat-treated alloys. A similar systematic investigation regarding creep properties of the alloys of Fe<sub>3</sub>Al-type was missing. To bridge this gap, it was decided to study the compressive creep of Fe-27% Al with 3 and 5% of niobium as a complement to previous studies of the alloys with 1% [19] and 10% Nb [17].

## 2. Materials and Methods

The alloys were prepared using vacuum induction melting and casting under Argon. The casts (dimensions 40 × 30 × 80 to 90 mm<sup>3</sup>), were rolled at 1200 °C to 13 mm in several steps, with a 15% thickness reduction in each pass. The composition of the investigated material was determined by wet chemical analysis and is given in Table 1 and marked in a part of the ternary Fe-Al-Nb diagram in Figure 1 [20]. The mean concentration of the technological impurities coming from the metals used for the preparation of the alloys was: 0.1% Cr, 0.01% B, 0.1% Mn, and 0.06% C. The results of the microstructure investigations are described in the previous paper [21]. The grains of the FA3Nb alloy

are large and have an irregular shape; their size is 200 to 500  $\mu\text{m}$ . The precipitates are  $\lambda_1$  Laves phase (C14)  $(\text{Fe, Al})_2\text{Nb}$ . These appear as smaller irregular shapes up to 10  $\mu\text{m}$  and as needle-like up to 50  $\mu\text{m}$  long. They are homogeneously distributed both along the grain boundaries and inside the grains. The grains of the FA5Nb alloy are coarse with dimensions in the order of hundreds of micrometers. The Laves phase forms a eutectic with the  $\text{Fe}_3\text{Al}$  matrix and comprises about 0.4 volume fractions of the eutectic.

**Table 1.** Chemical composition of the studied alloys (at. %).

Alloy	Fe	Al	Nb
FA3Nb	71.5	25.8	2.7
FA5Nb	67.9	27.3	4.8

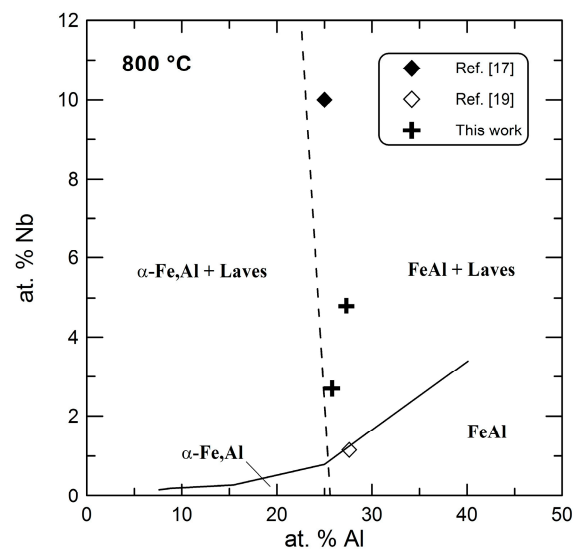


**Figure 1.** Detail of the isothermal section of the Fe-Al-Nb system at 800 °C according to Palm [20].

Creep tests were performed in uniaxial compression mode on prismatic samples with a height (gauge length) of 8 mm and a square base of cross-section  $4 \times 4 \text{ mm}^2$ . The samples were prepared by traveling wire electro-discharge machining and fine grinding of the contact surfaces. The tests were performed on a dead-weight creep machine that was constructed in-house in a protective atmosphere of dry purified argon. The load was applied in a perpendicular direction to the bases. The samples were subjected to stepwise loading, where the magnitude of the load was changed after a steady creep rate was established for a given load. A substantial amount of strain occurred before a constant creep rate was registered after each loading step. The terminal values of the true stress and the creep rate, i.e., the true compressive strain rate, were evaluated for each step:

$$\sigma_i = \frac{F_i l}{S_0 l_0} \quad (1)$$

$$\varepsilon = -\ln(l/l_0) \quad (2)$$

where  $F_i$  is the force applied in the  $i$ -th step,  $S_0$  is the initial cross-section area, and  $l$  and  $l_0$  are the instantaneous specimen height and the initial specimen height, respectively. The creep rate was found by linear fitting of the creep strain vs. the time curve in the linear part of the respective step. Figure 2 shows several examples that document how the creep strain evolves with time after both stress decrement and increment. Final deformation of the specimens was as a rule less than 0.1. The longest test duration was approximately 727 h; the total test duration was more than 3300 h.

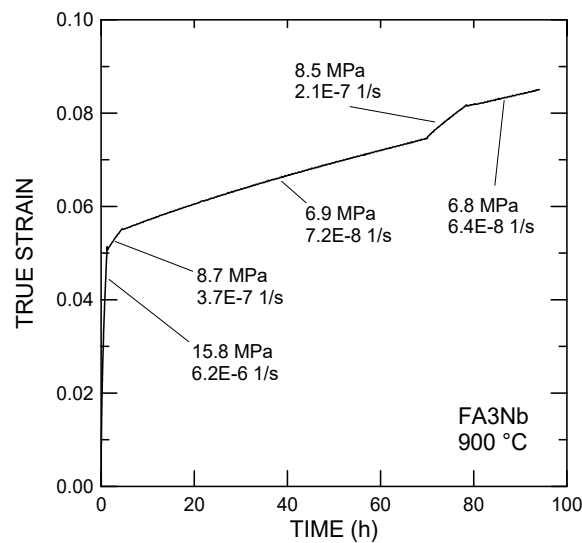


**Figure 2.** Example of a creep curve of the FA3Nb alloy at 900 °C showing five different segments with corresponding applied stresses and creep rates.

### 3. Results

The dependence of the creep rate  $\dot{\epsilon}$  on the applied stress  $\sigma$  at the various temperatures is shown in Figures 3 and 4, on a double logarithmic scale. The data were analyzed using the following relation:

$$\dot{\epsilon} = A\sigma^n \quad (3)$$

where  $A$  is a parameter dependent on the temperature and, and  $n$  is the stress exponent. Its values for both investigated alloys are summarized in Figure 5. The exponent  $n$  is, albeit slightly, dependent on the temperature. It should be noted that the same temperature dependence of  $n$  is evident for the alloy Fe-Al-Nb studied by Milenkovic and Palm [17]. A detailed analysis of the exponent  $n$  is possible provided a single mechanism is rate-controlling over the experimental range of stress and temperature. The effect of the mechanism change can be taken into account through an explicit dependence of the exponent  $n$  on stress [22]. In the studied alloys, the presence of Laves phase particles introduces threshold stress responsible for an apparent increase of the exponent  $n$  at lower stresses and consequently at higher temperatures [23].

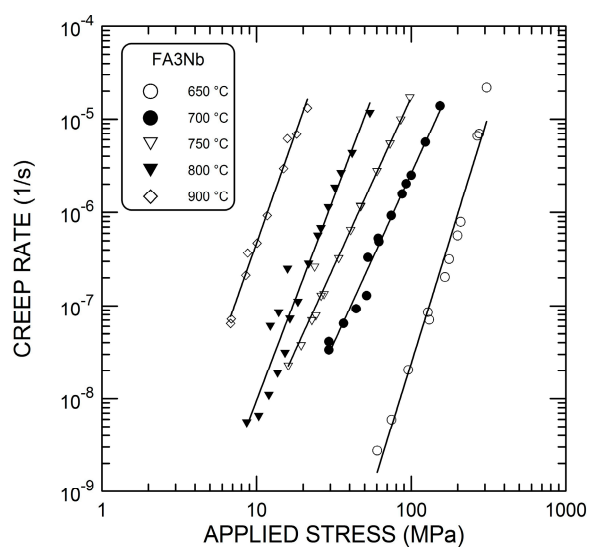


**Figure 3.** Dependence of the creep rate of the FA3Nb alloy on applied stress.

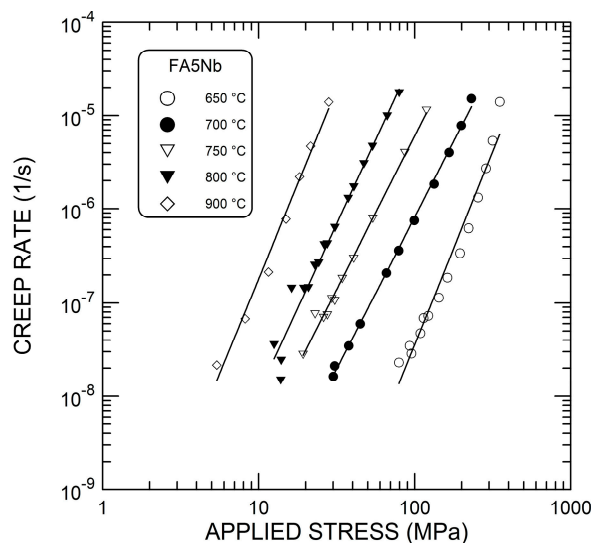


Figure 4. Dependence of the creep rate of the FA5Nb alloy on applied stress.

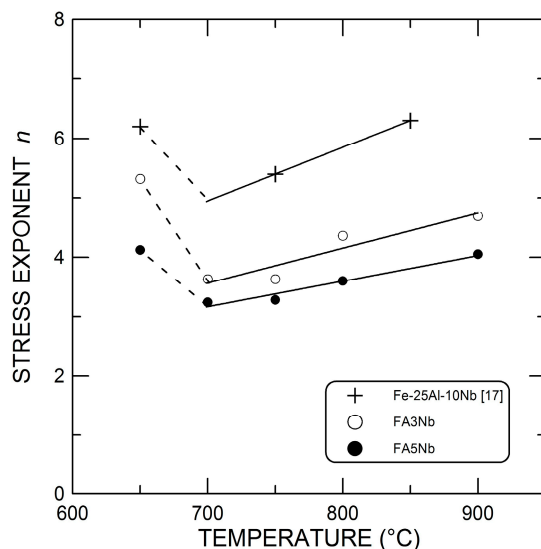


Figure 5. Dependence of stress exponent  $n$  on temperature.

To allow an approximate description of this behavior, the studied range of temperatures is formally divided into two areas: below and above 700 °C. Taking into account the ternary diagram, the proposed division results from a difference in the lattice structure: there would then be a  $D0_3$  lattice at 650 °C, and a  $B2$  lattice at 700 °C and above. Although the addition of niobium increases the temperature of the phase transition, the question is whether the niobium solubility is large enough to shift the transition to temperatures above 650 °C.

Relations between steady-state creep rate, and reciprocal temperature as derived from the  $\dot{\epsilon}$  vs.  $\sigma$  relations are shown in Figures 6 and 7. As in the above case of the stress exponent, we can also use the division into two temperature regions here. The apparent creep activation energy, defined as:

$$Q = - \left[ \frac{\partial \ln \dot{\epsilon}}{\partial (1/RT)} \right]_{\sigma}, \quad (4)$$

where  $T$  is the absolute temperature, and  $R$  is the universal gas constant, can be determined separately for both regions, although this determination should be taken with great caution at temperatures below 700 °C. The estimated activation energies for the high-temperature region are given in Figure 8.

The activation energy is close to 335 kJ/mol reported by McKamey et al. [11] for the Fe-28Al-1Nb alloy. It is also comparable to the activation enthalpy of the diffusion of the niobium in Fe(Al) as estimated by Morris et al. [24], i.e., 330 kJ/mole.

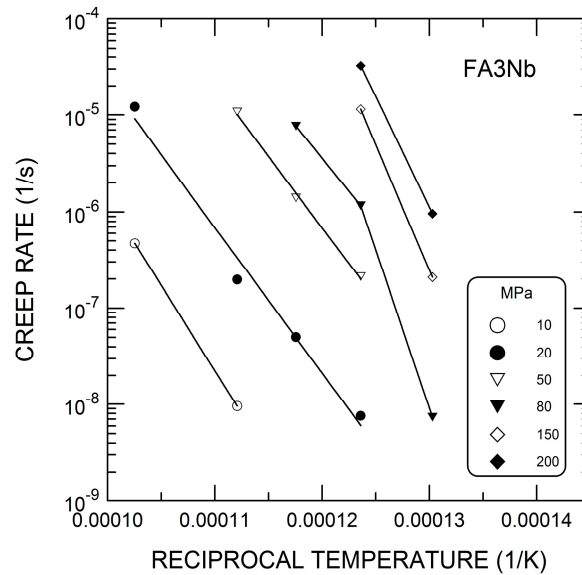


Figure 6. Dependence of minimum creep rate on reciprocal temperature for the alloy FA3Nb.

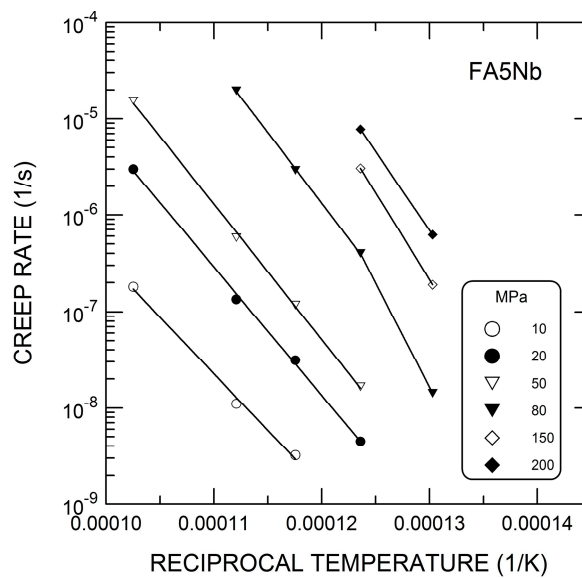


Figure 7. Dependence of minimum creep rate on reciprocal temperature for the alloy FA5Nb.

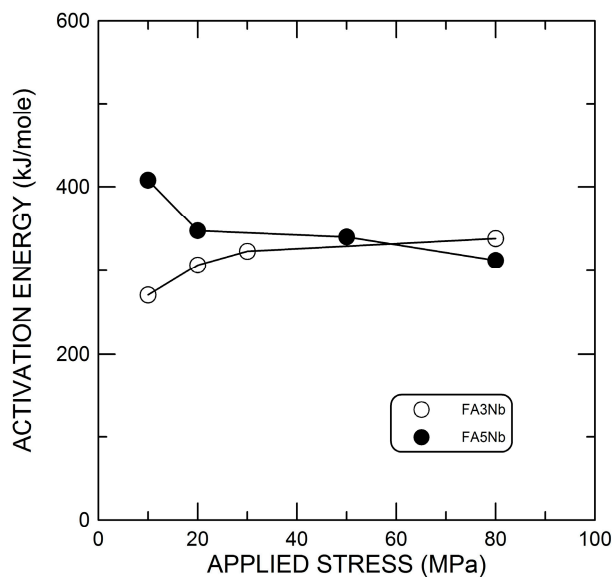


Figure 8. Dependence of activation energy  $Q$  on applied stress.

#### 4. Discussion

Figure 9 gives the selected creep data for the present FA3Nb alloy as well as data for the alloy with 1% of niobium [19], acquired also by compressive testing in the same laboratory, for tests over a range of identical temperatures. The figure confirms that the alloy with the lower niobium content is weaker than the alloy tested in the present study, at least at high creep rates. In the alloy with 1% of Nb, probably all the niobium is dissolved in the matrix, and the formation of the Laves phase is not expected.

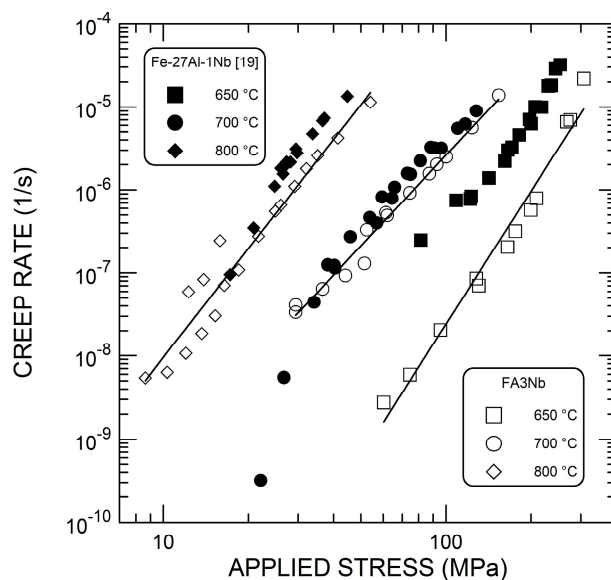
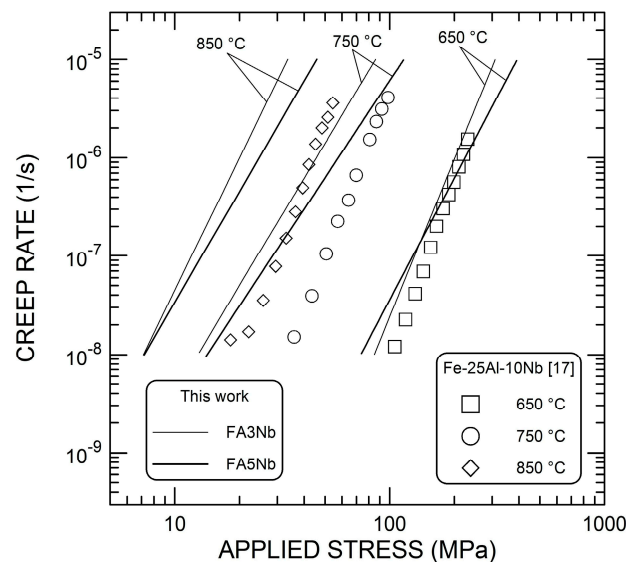


Figure 9. Comparison of the creep rate variation with the applied stress for the present alloy FA3Nb and Fe-Al-based alloy containing 1% of Nb [19].

For comparison with a previously published study on the Fe-25% Al alloy that contained the amount of niobium close to the eutectic composition [17], Figure 10 shows the creep rate vs. the stress data obtained at three temperatures. It has to be emphasized that the data in [17] were obtained by the identical testing technique, i.e., by the stepwise compressive testing. The lines for the present alloys

at a temperature of 850 °C were obtained by interpolation. Two different features follow from the comparison of the data:

- (i) At higher temperatures and lower stresses, the creep resistance of the 10% niobium alloy is higher than that of the lower niobium alloys. At a temperature of 850 °C, the creep resistance of the alloy with 10% of niobium is the best over the entire stress range studied.
- (ii) This effect is reversed at lower temperatures and higher stresses. At a temperature of 650 °C and stresses higher than 200 MPa, the 5% niobium alloy has the highest creep resistance.



**Figure 10.** Comparison of the creep rate variation with the applied stress for the present alloys and Fe-Al-based eutectic alloy containing 10% Nb addition [17].

In this regard, our results fully agree with the findings of Yildirim et al. [18], whose tests were conducted at room temperature and strain rate  $10^{-4} \text{ s}^{-1}$ . They observed a similar weakening of the heat-treated eutectic alloy and attributed lower compressive strength and fracture strain of this alloy to the absence of softer Fe-Al-based primary dendrites. From the point of view of the present results, the effect can be envisaged as follows: the eutectic alloy with 10% of niobium is weaker at high strain rates, but shows a steeper dependence of creep rate on stress, i.e., higher stress exponent  $n$ , such that the alloy maintains its strength better at slow strain rates.

## 5. Conclusions

The creep rates of the two Fe-27 at. % Al-based alloys with additions of niobium was studied in the temperature range from 650 °C to 900 °C. The stress exponent and the apparent activation energy were estimated. The following conclusions regarding the creep resistance of the alloy could be drawn:

- The studied range of temperatures could be divided into two areas: below and above 700 °C. This division follows the existence of different crystal lattices at lower and higher temperatures.
- The stress exponent  $n$  decreases with increasing temperature at temperatures up to 700 °C and increases at higher temperatures.
- The apparent activation energy of the creep is close to 335 kJ/mol and is comparable to the activation enthalpy of niobium diffusion in Fe(Al).
- At higher temperatures and lower stresses, the creep resistance of both alloys is worse than that of a 10% niobium eutectic alloy.
- At a temperature of 650 °C and stresses higher than 200 MPa, the 5% niobium alloy has the best creep resistance.

**Author Contributions:** F.D. performed the creep tests and wrote the paper, P.D. performed the creep tests, and M.F. conceived the research.

**Funding:** This research was funded by the Czech Science Foundation, grant number 17-22139S.

**Acknowledgments:** The authors wish to thank P. Kratochvíl (Charles University, Prague, Czech Republic) and V. Vodičková (Technical University, Liberec, Czech Republic) for the supply of the experimental alloys.

**Conflicts of Interest:** The authors declare no conflict of interest.

## References

1. Sauthoff, G. *Intermetallics*; VCH Verlagsgesellschaft: Weinheim, Germany, 1995; pp. 84–89.
2. Stoloff, N.S. Iron aluminides: Present status and future prospects. *Mater. Sci. Eng. A* **1998**, *258*, 1–14. [[CrossRef](#)]
3. Liu, C.T.; George, E.P.; Maziasz, P.J.; Schneibel, J.H. Recent advances in B2 iron aluminide alloys: Deformation, fracture and alloy design. *Mater. Sci. Eng. A* **1998**, *258*, 84–98. [[CrossRef](#)]
4. Palm, M. Concepts derived from phase diagram studies for the strengthening of Fe–Al-based alloys. *Intermetallics* **2005**, *13*, 1286–1295. [[CrossRef](#)]
5. Morris, D.G.; Muñoz-Morris, M.A. Development of creep-resistant iron aluminides. *Mater. Sci. Eng. A* **2007**, *462*, 45–52. [[CrossRef](#)]
6. Baligheid, R.G. Effect of niobium on microstructure and mechanical properties of hot-rolled Fe-8.5 wt% Al-0.1 wt% C alloy. *J. Mater. Sci.* **2004**, *39*, 5599–5602. [[CrossRef](#)]
7. Baligheid, R.G. Effect of niobium on microstructure and mechanical properties of high carbon Fe–10.5 wt.% Al alloys. *Mater. Sci. Eng. A* **2004**, *368*, 131–138. [[CrossRef](#)]
8. Morris, D.G.; Muñoz-Morris, M.A.; Requejo, L.M.; Baudin, C. Strengthening at high temperatures by precipitates in Fe–Al–Nb alloys. *Intermetallics* **2006**, *14*, 1204–1207. [[CrossRef](#)]
9. Morris, D.G.; Requejo, L.M.; Muñoz-Morris, M.A. Age hardening in some Fe–Al–Nb alloys. *Scripta Mater.* **2006**, *54*, 393–397. [[CrossRef](#)]
10. Morris, D.G.; Muñoz-Morris, M.A. Room and high temperature deformation behaviour of a forged Fe–15Al–5Nb alloy with a reinforcing dispersion of equiaxed Laves phase particles. *Mater. Sci. Eng. A* **2012**, *552*, 134–144. [[CrossRef](#)]
11. McKamey, C.G.; Maziasz, P.J.; Jones, J.W. Effect of addition of molybdenum or niobium on creep-rupture properties of Fe<sub>3</sub>Al. *J. Mater. Res.* **1992**, *7*, 2089–2106. [[CrossRef](#)]
12. McKamey, C.G.; Maziasz, P.J.; Goodwin, G.M.; Zacharia, T. Effects of alloying additions on the microstructures, mechanical properties and weldability of Fe<sub>3</sub>Al-based alloys. *Mater. Sci. Eng. A* **1994**, *174*, 59–70. [[CrossRef](#)]
13. Zhang, Z.H.; Sun, Y.S.; Guo, J. Effect of niobium addition on the mechanical properties of Fe<sub>3</sub>Al-based alloys. *Scripta Metall. Mater.* **1995**, *33*, 2013–2017.
14. Yu, Y.Q.; Sun, Y.S. Improvement of creep resistance of Fe<sub>3</sub>Al based alloys with tungsten and niobium additions. *J. Mater. Sci. Lett.* **2001**, *20*, 1221–1223.
15. Morris, D.G.; Muñoz-Morris, M.A.; Baudin, C. The high-temperature strength of some Fe<sub>3</sub>Al alloys. *Acta Mater.* **2004**, *52*, 2827–2836. [[CrossRef](#)]
16. Falat, L.; Schneider, A.; Sauthoff, G.; Frommeyer, G. Mechanical properties of Fe–Al–M–C (M = Ti, V, Nb, Ta) alloys with strengthening carbides and Laves phase. *Intermetallics* **2005**, *13*, 1256–1262. [[CrossRef](#)]
17. Milenkovic, S.; Palm, M. Microstructure and mechanical properties of directionally solidified Fe–Al–Nb eutectic. *Intermetallics* **2008**, *16*, 1212–1218. [[CrossRef](#)]
18. Yildirim, M.; Vedat Akdeniz, M.; Mekhrabov, A.O. Microstructural evolution and room-temperature mechanical properties of as-cast and heat-treated Fe<sub>50</sub>Al<sub>50-n</sub>Nb<sub>n</sub> alloys ( $n = 1, 3, 5, 7, \text{ and } 9$  at%). *Mater. Sci. Eng. A* **2016**, *664*, 17–25. [[CrossRef](#)]
19. Dobeš, F.; Kratochvíl, P.; Pešička, J.; Vodičková, V. Microstructure and creep behavior of Fe–27Al–1Nb alloys with added carbon. *Metal. Mater. Trans. A* **2015**, *46*, 1580–1587. [[CrossRef](#)]
20. Palm, M. Phase equilibria in the Fe corner of the Fe–Al–Nb system between 800 and 1150 °C. *J. Alloys Compd.* **2009**, *475*, 173–177. [[CrossRef](#)]
21. Kratochvíl, P.; Švec, M.; Král, R.; Veselý, J.; Lukáč, P.; Vlasák, T. The effect of Nb addition on the microstructure and the high-temperature strength of Fe<sub>3</sub>Al aluminide. *Metal. Mater. Trans. A* **2018**, *49*, 1598–1603. [[CrossRef](#)]

22. Bonora, N.; Esposito, L. Mechanism based creep model incorporating damage. *J. Eng. Mater. Technol.* **2010**, *132*, 021013. [[CrossRef](#)]
23. Esposito, L.; Bonora, N.; De Vita, G. Creep modelling of 316H stainless steel over a wide range of stress. *Procedia Structural Integrity* **2016**, *2*, 927–933. [[CrossRef](#)]
24. Morris, D.G.; Muñoz-Morris, M.A.; Requejo, L.M. New iron–aluminium alloy with thermally stable coherent intermetallic nanoprecipitates for enhanced high-temperature creep strength. *Acta Mater.* **2006**, *54*, 2335–2341. [[CrossRef](#)]



© 2019 by the authors. Licensee MDPI, Basel, Switzerland. This article is an open access article distributed under the terms and conditions of the Creative Commons Attribution (CC BY) license (<http://creativecommons.org/licenses/by/4.0/>).